Copyright Information

Floating Underwater Manipulation: Developed Control Methodology and Experimental Validation within the TRIDENT Project

Enrico Simetti
ISME: Interuniversity Center on
Integrated System for the Marine Environment
University of Genova
Genova, Via Opera Pia 13
simetti@dist.unige.it

Giuseppe Casalino
ISME: Interuniversity Center on
Integrated System for the Marine Environment
University of Genova
Genova, Via Opera Pia 13
casalino@dist.unige.it

Sandro Torelli
ISME: Interuniversity Center on
Integrated System for the Marine Environment
University of Genova
Genova, Via Opera Pia 13
sandro.torelli@unige.it

Alessandro Sperindé
ISME: Interuniversity Center on
Integrated System for the Marine Environment
University of Genova
Genova, Via Opera Pia 13
alessandro.sperinde@unige.it

Alessio Turetta
ISME: Interuniversity Center on
Integrated System for the Marine Environment
University of Genova
Genova, Via Opera Pia 13
alessio.turetta@unige.it

Abstract

The paper presents the control framework which has been proposed and successfully employed within the TRIDENT EU FP7 project, whose aim is to develop a multipurpose

I-AUV (Intervention Autonomous Underwater Vehicle) exhibiting smart manipulation capabilities, for interventions within unstructured underwater environments. In particular, the work focuses on the exploitation of the highly redundant system for achieving a dexterous object grasping, while also satisfying a set of conditions of scalar inequality type to be achieved ultimately. These represent safety and/or operational-enabling conditions for the overall system itself, such as for instance respecting joint limits and keeping the object grossly centered in the camera system. Thus the design of a control architecture exhibiting such a property first required an extension of the classical task priority framework, to be performed in such a way to also account, in uniform manner, for inequality conditions to be achieved ultimately. Then, following a description on how such an extension has been made, both simulations and experimental trials are successively presented for showing how the developed TRIDENT I-AUV system is able to properly exploit all the redundant d.o.f. for achieving all the established objectives.

1 Introduction

Nowadays, highly redundant robotic structures have become far more common than a few decades ago. Such robots can be redundant manipulators, manipulators mounted on mobile or even free-floating platforms, humanoid robots, snake robots and so on. At the same time, the computational power available to control such systems has scaled from the 32MHz Motorola 68040 CPUs that were used to control the dual arm work cell developed within the pioneering project AMADEUS [Lane et al., 1997], where the computation of a 6×7 pseudo-inverse [Ben-Israel and Greville, 2003] required around $150ms$, to dual or quad core GHz systems where instead the same operation now takes a few microseconds.

The control of such redundant systems is thus a challenging and very active topic of research. Indeed, the work presented in this paper derives its motivation from the EU-FP7 funded project TRIDENT, whose aim is to develop a multipurpose I-AUV (Intervention Autonomous Underwater Vehicle) exhibiting smart manipulation capabilities, to be used for interventions within unstructured underwater environments [**?**]. Figure 1 shows the full system engaged in one of the preliminary pool trials.

As stated by the relevant documents, "the TRIDENT project is built on the top of two main concepts: 1) the use of a team of heterogeneous marine robots with complementary skills; namely an USV (Unmanned Surface Vehicle) and an I-AUV, to achieve light intervention capabilities without the need for expensive

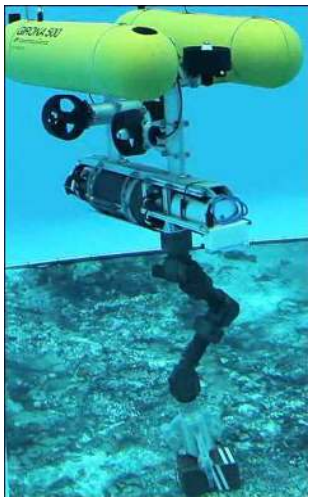

Figure 1: The TRIDENT I-AUV system, encompassing the University of Girona G500 vehicle, the Graal Tech 7 d.o.f. underwater electrical arm and the University of Bologna dexterous hand (photo courtesy of the TRIDENT consortium)

support ships; and 2) the use of a dexterous hand, mounted on the redundant robot arm endowing the I-AUV, to achieve multipurpose manipulation capabilities".

After the first phase where a survey of the seafloor area of interest is conducted by the USV and the I-AUV cooperatively navigating approximately one upon the other, a geo-referenced object of interest is located by the user on the computed acoustic/optical map provided by the I-AUV, once returned and docked with the USV. Then in the second phase the I-AUV is made to navigate toward the approximate object location, where it starts to autonomously search for it within a small seafloor area. Once the object is eventually located, it must be then autonomously grasped and recovered from the seafloor by the I-AUV itself.

It is at this point that the highly redundant system (6 d.o.f. for the free-floating vehicle, and 7 d.o.f. arm) must be suitably coordinated for achieving the object grasping and its successive transportation. Aside from the primary objective of the mission, i.e. the recovery of the object, which translates into a position control for the end-effector of the arm, the system must also take care of many other objectives. Obviously, the arm's joint limits must be respected, and the singularity postures of the arm must be avoided. Moreover, since the estimate of the object position w.r.t. the vehicle frame is provided by a stereo camera mounted on the vehicle, another important objective is to keep the object grossly centered inside the stereo camera visual cone, otherwise the feedback would be lost and the search for the object would need to start again. Also, the object should be at a certain horizontal and vertical distance from the camera frame, in order for the vision algorithm to perform well. Finally, the vehicle should be kept within reasonable roll and pitch angle values.

With the exception of the position control of the end-effector, which is clearly an equality condition to be achieved ultimately, all the other control objectives are instead represented by scalar inequality constraints involving different system variables, to be also achieved ultimately. Consequently this justifies the interest and the research efforts which have been spent by the authors to pursue a simple and effective way to incorporate all these inequality and equality objectives into a unifying, task-priority based, framework for the control of redundant robotic structures. And this work will therefore solely focus on the control and coordination aspects that were employed in the TRIDENT project.

Within the TRIDENT project other key aspects have been developed by other partners, including for instance the object pose estimation via vision, the planning of the grasp and the dexterous manipulation via multi-sensory integration. However, such additional important aspects will not be covered in this paper, since it is solely focused on the arm-vehicle control and coordination aspects encountered within the overall TRIDENT project developments.

As regards the specific topics of this paper, an extensive formulation of the supporting theory can be found in one of the technical reports of the TRIDENT project [Casalino, 2011] even if it will be duly recalled here. Moreover, preliminary simulations were already presented in [Casalino et al., 2012a, Casalino et al., 2012b], while additional ones, then followed by physical experimental field trials, will be presented and discussed within this work.

As a consequence this work is organized as follows: related works and the main contribution of this paper are summarized in Section 2. Section 3 recalls the proposed unifying framework for handling equality and inequality objectives. Then, in Section 4, the established framework is further reformulated in a more efficient form which manages the arm and the vehicle as cooperative agents, while also introducing some other interesting advantages related to both multi-rate sampling management and disturbance rejection. Section 5 introduces the overall architecture employed within the TRIDENT project, composed of two separate layers: the first one, at kinematic level, exploiting the proposed task priority approach, while the second one takes care of the dynamic control aspects. Then, additional simulation results supporting the proposed approach are presented in Section 6, while Section 7 shows the experimental results obtained with the physical I-AUV, formerly at the University of Girona pool and then at Port Sòller Harbour in the isle of Majorca, Spain. Finally, conclusions and future research trends are given in Section 8.

2 Related Works

Control of floating manipulation structures has been the focus of different studies during the late 80s, especially in the field of space robotics, leading to important results in hierarchical control architectures [Aikenhead et al., 1983,Albus et al., 1988,Spofford and Akin, 1990,McCain et al., 1991,Andary and Spidaliere, 1993] and the definition of a standard reference model for telerobot control system architecture [Albus et al., 1989]. However, in most of these works the coordination aspects were treated considering the global dynamic model of the system.

As regards the underwater domain, during early 90s seminal works have been carried out at the Woods Hole Oceanographic Institute concerning the design and control compliant underwater manipulators [Yoerger et al., 1991] and the coordinated vehicle/arm control for tele-operation [Schempf and Yoerger, 1992], while the first successful attempts at underwater autonomous intervention were obtained within the SAUVIM project [Yuh et al., 1998]. A nice survey on the developed control architectures for underwater robots until late 90s can be found in [Yuh, 2000].

The exploitation of redundancy at kinematic level dates back to the early works [Yoshikawa, 1984], [Macjeiesky and Klein, 1985], where the problems of singularity avoidance and obstacle avoidance for an industrial manipulator were tackled. In such works the inequality constraints were treated as equality ones. This was done by imposing the achievement of an arbitrary fixed point located inside the validity of the inequality objective (and by performing this achievement within the null-space of the primary task, represented by a trajectory tracking for the end-effector).

A more precise formulation of the task-priority framework then appeared in [Nakamura, 1991] for two equality tasks; which was later generalized to any number of equality tasks within the seminal work [Siciliano and Slotine, 1991], where each prioritized task was therefore imposed to be satisfied within the null space of all its preceding higher priority ones.

Since those times, the task-priority framework has been applied to numerous robotic systems: redundant manipulators, as was obvious in each of the works mentioned until now; mobile manipulators such as [Antonelli and Chiaverini, 1998], [Antonelli and Chiaverini, 2003], [Casalino and Turetta, 2003], [Han and Chung, 2007], [Marani et al., 2008]; multiple coordinated mobile manipulators [Padir, 2005], [Simetti et al., 2009]; and also humanoid robots [Sentis and Khatib, 2005], [Sugiura et al., 2007] just to cite a few examples. In particular, in some of these works, the problem of the achievement of inequality objectives was also tackled

via ad-hoc solutions [Casalino and Turetta, 2003, Simetti et al., 2009].

In a very recent paper [Kanoun et al., 2011] a framework for handling a hierarchy of both equality and inequality objectives is proposed (generalizing the earlier work [Faverjon and Tournassoud, 1987]), where for each of the inequality objectives the cumbersome solution of a set of constrained quadratic problems is required. In their paper [Kanoun et al., 2011], the authors also remark again how, within the previous works concerning the task-priority framework, the presence of inequality constraints was never systematically tackled whilst preserving their true meaning, because they were so often replaced by more restrictive equality objectives, arbitrarily chosen inside the validity of the inequality ones, causing an over-constraining problem for the robotic system in hand. This last fact has been consequently used for fostering their proposed solution as a possible definitive one.

The remark provided in [Kanoun et al., 2011] is quite correct whenever the translation into equality objectives is explicitly performed. However, it is the opinion of the authors of this paper that the same remark becomes questionable (at least partially) whenever smooth potential fields, exhibiting a null support over the region where the inequality is satisfied, are instead used for representing inequality objectives; as for example it was just done in the mentioned works [Casalino and Turetta, 2003,Simetti et al., 2009]. The use of finite-support smooth potential fields for representing inequality objectives is what is re-proposed here, now in a systematic way, via the use of the so-called activation functions that will be presented in Section 3.4. And in this way the criticism embedded in the above recalled remark consequently ceases to exist, since the translation of the inequality objectives into restrictive equality ones is not at all performed anymore.

However, as it has been also remarked in [Mansard et al., 2009a] and in more details in [Mansard et al., 2009b], with the use of the activation functions there might still be problems related to the rapidity of variation (even if with continuity) of the associated solutions, with possible resulting chattering phenomena around the activation thresholds, in case of not sufficiently small sampling times. However such claims cease to be valid whenever the involved pseudo-inversions are performed with suitably chosen smooth regularization factors, as it will be shown in Section 3.4.

The above considerations represent the core ideas supporting the present work, where a framework for task-priority control encompassing both equality and scalar inequality objectives is presented. The proposed approach extends the early work [Siciliano and Slotine, 1991] by introducing the inequality constraints and simplifying the method for the null-space projection (since it does not require to stack all the previous Jacobian matrices). Moreover, the proposed framework also results computationally simpler than [Kanoun

et al., 2011], since it is based on the solution of a sequence of linearly constrained least square problems, rather than on the solution of a sequence of least square problems with linear inequality and equality constraints of increasing dimensions, which is computationally more expensive.

As already stated, a second contribution of this work is represented by the extension of the general task-priority based framework to the case when the arm and the vehicle are considered as separate interacting and cooperating agents. Such an extension, which is built on previous works of the authors [Casalino and Turetta, 2003], [Casalino et al., 2009], exploits DP techniques suitably made running, at each sampling instant, along the arm-vehicle kinematic chain, in order to achieve optimal coordination between the two subsystems. Such an approach has different benefits, when compared to a centralized one, for various reasons: i) it allows to deal in an easier manner with multi-rate sampling situations; ii) it simplifies the integration of heterogeneous lower-level controllers possibly provided by different companies or project partners.

3 Task-Priority Based Coordinated Control for Floating Manipulation

In this section, the theoretical foundations supporting the task priority based control and coordination framework developed within the TRIDENT project will be presented. First, an introduction to task-prority control and the proposed architecture is given in subsection 3.1. After that, the various control objectives (of inequality and/or equality type) will be specified in subsection 3.2; then some useful formal definitions of general use will be given in subsection 3.3; and finally the developed task priority based framework will be presented in subsections 3.4 to 3.6.

3.1 Introduction

Before entering into mathematical details, it is worth starting the dissertation by introducing the considered scenario and the general idea underlying the proposed control framework.

The TRIDENT robotic system is asked to achieve multiple objectives of different nature, each one consisting in having a quantity of interest ultimately equal to a target value, or included within a target set of values. An example of the first type is having the arm end-effector precisely reach a goal frame; while one of the second type is the vehicle keeping the object to be grasped within the field of view of the onboard camera. In such a scenario, the control problem is therefore that of 1) tracking at best a suitable reference rate, capable of

individually driving the associated variable toward the corresponding objective, for each variable of interest (this is typically termed as task); and simultaneously, 2) translating the set of tasks into a corresponding set of system velocity references (i.e. the arm joint velocities and vehicle linear and angular velocities) to be provided to the low-level actuators in such a way to maximally achieve all the objectives.

A necessary condition for having all the objectives achieved ultimately is the existence of a non-void set of system configurations, to be eventually reached by the system, where all the objectives are contemporaneously satisfied. The presence of such a *non-conflicting zone* is, however, not a sufficient condition, as it does not imply its reachability in correspondence of all system initial configurations starting outside it.

Finding out the conditions guaranteeing the fulfillment of the above two properties represents an interesting problem in general, certainly deserving deeper investigations, which are however outside the scope of the present work, since, for the TRIDENT system in hand, preliminary extensive geometric simulations and trials performed during its design phase actually guarantee their fulfillment.

However, despite the fulfillment of the above conditions, it might still happen that, when the system is outside the non-conflicting zone, at certain time instants two or more tasks may result conflicting each other; thus possibly leading to scarcely controllable dead-lock situations, which might in turn make difficult (if not even impossible) reaching the non-conflicting zone.

As a consequence, a policy must be devised for suitably combining all the tasks. To this aim, the task-priority paradigm [Nakamura, 1991, Siciliano and Slotine, 1991], where a priority can be assigned to each task according to its given importance, has been selected as a basis for the present work.

Once the priorities have been defined, at any time interval, tasks are solved following their priority in a descending order: the highest priority task is solved first, and then the solution of each task is searched inside the subspace of the solutions of all the preceding, higher priority ones. In this way the achievement of a task is never affected by the lower priority ones.

Despite its benefits, a limit of the original task-priority framework formulation was that only equality objectives were considered, like in the case of the end-effector goal reaching task, where the position and attitude of the arm end-effector has to exactly become *equal* to its assigned target frame. On the contrary, an inequality objective like for instance the joints limits avoidance (and many others, as in Section 3.2), which can be considered accomplished whenever the joints values are *lower than* a certain safety threshold from their limits, was not contemplated.

As a consequence, every inequality objective, in order to be introduced, had always to be preliminarily transformed into an equality one, by assigning an arbitrary target point for the quantity of interest inside the solution region of the original inequality. By doing so, however, a task velocity reference was always imposed to the system, even when the corresponding original inequality was satisfied. The task related to inequality objective was therefore maintained always active, with the consequent risk of over-constraining the system even when not necessary [Yoshikawa, 1984, Macjeiesky and Klein, 1985, Casalino and Turetta, 2003, Simetti et al., 2009].

An important contribution of the present work is the extension of the original framework by encompassing also scalar inequality objectives in a very simple way. Every task related to an inequality is added with the use of a so called *activation function*, which smoothly deactivates the task whenever its related inequality condition becomes satisfied. By doing so, when the task disappears from the priority list, this induces an enlargement of the system mobility space, which is in turn favorable to the progress of the other lower priority tasks.

Therefore, within this framework, it becomes possible to efficiently consider tasks related with objectives regarding the system safety and/or its good operational conditions, which are generally described by inequality objectives. Further, as they can be assigned a priority higher than those of equality type, all safety and good operational conditions requirements can therefore be achieved and maintained as soon as possible within the overall set of system activities. In this way the final accomplishment of the equality tasks can be then obtained in an easier and safer way, as it has been actually done within the TRIDENT project.

We can conclude the present introduction by finally remarking that in TRIDENT each task related with inequality objective is assigned to a distinct priority level, i.e. activities regarding the achievement of inequality objectives are never performed with the same priority. This leads to deal only with scalar inequality objectives. As we shall see such a choice revealed a suitable mean for avoiding possible discontinuities in the control solutions that might otherwise arise in the opposite case (see [Mansard et al., 2009a, Mansard et al., 2009b] for a deep discussion). Furthermore, it is also much simpler and effective for the TRIDENT system than the quite general, but more complex procedure that was proposed in [Mansard et al., 2009b].

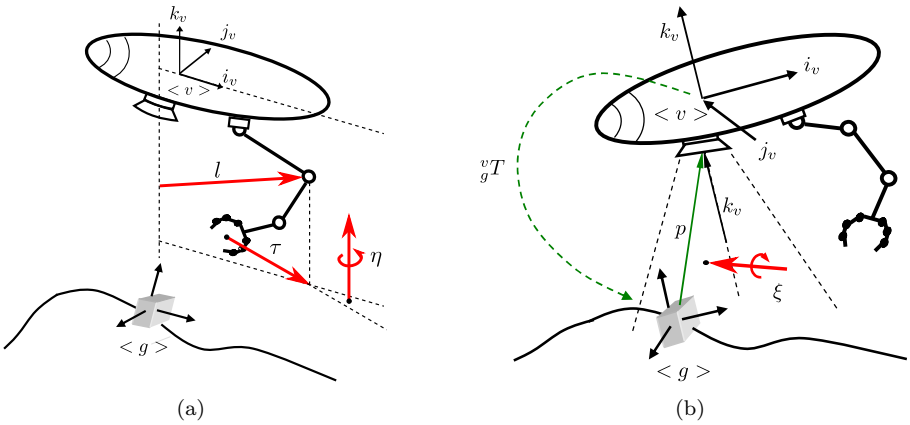

Figure 2: (a) camera occlusion task (b) camera centering task

3.2 Control Objectives

One of the main objectives, of an inequality type, related to both the safety and operability of the arm is that of maintaining its joints within well defined bounds for each one of them, that is

$$q_{i,m} \leq q \leq q_{i,M} \; ; \; i = 1, \ldots, 7, \tag{1}$$

where the subscript m will be used to indicate minimum values, while subscript M will instead refer to maximum ones.

Moreover, in order to guarantee the arm operating with a good dexterity, the arm itself must also keep its manipulability measure [Yoshikawa, 1985] above a minimum value, thus leading to the following inequality type objective

$$\mu \geq \mu_m. \tag{2}$$

While the above objectives arise from inherently scalar variables, other ones instead arise from conditions to be achieved within the Cartesian space, where each one of them can be conveniently expressed in terms of the modulus associated to a corresponding Cartesian vector variable.

To be more specific, let us for instance start referring to the necessity of avoiding the occlusions between the object and the stereo-camera endowing the vehicle, which might occasionally occur due to motions of the arm links. Such need can be formalized by requiring the ultimate achievement of the following set of

inequalities, for suitable chosen values of the boundaries

$$\|l\| > l_m \tag{3}$$

$$\|\tau\| > \tau_m \tag{4}$$

$$\|\eta\| < \eta_M \tag{5}$$

where l is the vector lying on the vehicle $x-y$ plane, joining the arm elbow with the line parallel to the vehicle z-axis and passing through camera frame origin, as indicated in Fig. 2(a). Moreover η is the misalignment vector formed by vector τ, it also lying on the vehicle $x-y$ plane, joining the lines parallel to the vehicle z-axis and respectively passing through the elbow and the end effector origin, as it also appears indicated in the same figure. For avoiding possible ill-definitions of η, it is assumed τ starting from a non-zero value allowing the definition of its unit vector (such initial easy maneuvering is unfortunately unavoidable).

Given the specific configuration of the TRIDENT system, and confirmed by the preliminary experimental trials, most camera occlusions are due to the arm elbow. Thus, a simplified method to limit the occlusions is to only prevent the elbow from entering the cone of view of the camera system. Such a requirement is translated in a boundary for the misalignment vector ψ that the vector joining the base of the arm to the elbow, projected on the vehicle horizontal plane, makes with the longitudinal axis of the vehicle:

$$\|\psi\| \leq \psi_M. \tag{6}$$

Such a simplified but effective choice is what has been used during the contingency of the field trials.

As for the vehicle, it must keep the object of interest grossly centered in the camera frame (see Fig. 2(b)). This means that the modulus of the orientation error ξ, formed by the unit vector n_p of vector p, joining the origin of the object to the camera frame, and the unit vector k_c of the z axis of the camera frame itself, must ultimately satisfy the following inequality

$$\|\xi\| < \xi_M. \tag{7}$$

Furthermore, the vehicle must also be closer than a given horizontal distance d_M to the vertical line passing through the object, and between a maximum and minimum height with respect to the object located on the

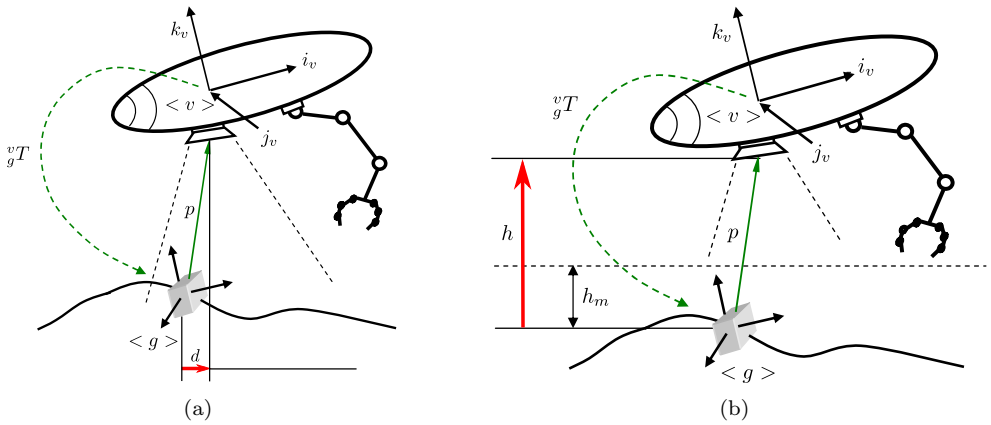

Figure 3: (a) camera distance task (b) camera height task

sea floor. This consequently translates into the requirement of achieving the following inequalities

$$\|d\| \leq d_M, \tag{8}$$

$$h_m \leq \|h\| \leq h_M, \tag{9}$$

where d and h are the horizontal and vertical vectors which appear respectively indicated in Fig. 3.

By proceeding further on, since the vehicle should also preferably stay at an almost horizontal attitude, this requires the achievement of the following additional inequality

$$\|\varphi\| \leq \varphi_m, \tag{10}$$

where φ represents the misalignment vector that the absolute vertical unit vector k_0 forms with respect to the vehicle z-axis one k_v.

Finally, within the fulfillment of the above goals, the end-effector must eventually reach the object frame, to then start the successive grasping phase. Thus the following, now of equality type, objectives also have to be achieved

$$\|r\| = 0 \;\; ; \;\; \|\vartheta\| = 0, \tag{11}$$

where r is the position error and ϑ the orientation error.

For the time being, let us conclude the present subsection by noting how, within the TRIDENT system, all the vectors involved in the above defined control objectives can be evaluated in real-time, with components on the vehicle frame, via the knowledge of the current arm posture and the transformation matrix of the object

frame with respect to the vehicle one, with real-time data provided by the stereo-vision system endowing the vehicle (see [Casalino, 2011] for more specific details).

3.3 Definitions

In this subsection some formal definitions are introduced, which shall be useful for the successive developments. To this aim let us denote a vector associated to a generic control objective defined in the Cartesian space as $s \in \mathbb{R}^M$ and term it as an error-vector. Then its module

$$\sigma \triangleq \|s\|, \tag{12}$$

will be termed as the error; while its unit vector

$$n \triangleq \frac{s}{\sigma} \; ; \; \sigma \neq 0, \tag{13}$$

will be termed as the unit error vector. Then, by taking into account that a generic error-vector is subjected to change under the action of the various system velocities, the following Jacobian relationship can therefore be evaluated for each error vector

$$\dot{s} = Hy, \tag{14}$$

where $y \in \mathbb{R}^N$ is the stacked vector composed of the joint velocity vector $\dot{q}$, plus the stacked vector v of the vehicle velocities, with components on the vehicle frame. Matrix $H \in \mathbb{R}^{M \times N}$ is therefore the Jacobian matrix relating y and $\dot{s}$, with the latter clearly representing the time derivative of vector s performed with respect to the vehicle frame and with components on it. Still refer to [Casalino, 2011] for a very detailed presentation on how each Jacobian matrices H can be evaluated in real-time in correspondence of each error-vector.

Instead, with regard to the time derivative $\dot{\sigma}$ of a generic error, the following holds:

$$\dot{\sigma} = n^T H y. \tag{15}$$

To each error variable σ, associated to a corresponding objective, let us also associate a so-called error reference rate $\dot{\bar{\sigma}}$ of the form

$$\dot{\bar{\sigma}} \triangleq -\gamma(\sigma - \sigma^o)\beta(\sigma), \tag{16}$$

where, for an equality objective, σ^o is the target point and $\beta(\sigma) \equiv 1$; while for a single-ended inequality

objective σ^o is the threshold value, and $\beta(\sigma)$ is a left-cutting or right-cutting binary function, in dependence of whether the objective is to force the error σ to be above or below the threshold σ^o, respectively. Double-ended inequality objectives are considered decomposed into two separate single-ended ones, for which the error rate assignments are separately provided.

It may be noted that, despite the presence of the binary function $\beta(\sigma)$, any error reference rate however results into a linear, or piecewise linear, continuous function of σ.

In case it could be exactly assigned to its corresponding error rate $\dot{\sigma}$, (16) would guarantee the achievement of the associated objective. However, for inequality objectives, it would consequently impose $\dot{\sigma} = 0$ to whatever point is located inside the interval of validity of the inequality objective itself. In correspondence of such inner points the error rate zeroing condition should instead be relaxed, just for allowing a system mobility increase which might be necessary (or at least helpful) for also achieving other control objectives. Such a relaxation aspect will be dealt with in subsection 3.4.

Let us also consider the so-called reference error-vector rate, directly associated to a reference error rate $\dot{\bar{\sigma}}$, as defined below,

$$\dot{\bar{s}} \triangleq n\dot{\bar{\sigma}}, \tag{17}$$

which trivially translates into the following, in correspondence of equality control objectives requiring the zeroing of error σ:

$$\dot{\bar{s}} = -\gamma s, \tag{18}$$

whose evaluation can be performed in a direct way (i.e. without the preliminary evaluation of the unit error vector n). As it will be clear in subsection 3.6, the use of the reference error rate (18) will reveal its importance for the management of equality objectives requiring the zeroing of their error variable.

3.4 Managing the Highest Priority Inequality Objective

Let us start by considering the highest priority task. Since, as mentioned before, such a task corresponds to a scalar inequality objective, the control action should drive the error σ_1 towards its validity interval (when σ_1 is outside) and should do nothing when the inequality condition is satisfied (when σ_1 is inside). From now on, to shorten the terminology, let us term such kind of tasks as *inequality tasks*.

To this aim, an intuitive idea for devising all system velocity vectors allowing such a possibility arises from

considering the linear manifold of solutions of the following linear quadratic optimization problem

$$\mathcal{S}_1 \triangleq \left\{ y = \arg\min_y \alpha_1^2 \left\| \dot{\tilde{\sigma}}_1 - n_1^T H_1 y \right\|^2 \right\}, \tag{19}$$

where $\dot{\tilde{\sigma}}_1$ is the error reference rate associated to the inequality objective, previously introduced in subsection 3.3; while α_1 is a suitable smooth activation function, that is a left or right window sigmoid function starting from the objective threshold σ_1^o, in dependence of whether the inequality objective is to force the error σ_1 to be above or below the objective threshold σ_1^o itself, respectively. The focus is set on the manifold, rather on the single minimum norm solution, because the arbitrariness in the solution will be exploited by the successive tasks.

Looking at (19) it is immediate to see that two main cases can be studied depending on the value of α_1, i.e. $\alpha_1 = 0$ and $\alpha_1 \neq 0$.

For $\alpha_1 \neq 0$ (even whatever small), it is easy to see that α_1^2 does not have any effect on the solution of (19). Thus, the corresponding solutions manifold is

$$y = \left(n_1^T H_1\right)^{\#} \dot{\tilde{\sigma}}_1 + \left[I - \left(n_1^T H_1\right)^{\#} \left(n_1^T H_1\right) \right] z_1 \;\; ; \;\; \forall z_1, \tag{20}$$

where the first term corresponds to the minimum norm solution, while the second term, parametrized by z_1 vector, represents the allowed arbitrariness within the solution, which will be successively used to perform all the subsequent tasks. The notation $(\cdot)^{\#}$ refers to the regularized pseudo inverse (see [Ben-Israel and Greville, 2003] for a complete review on pseudo inverses), which for a row vector (as it is $n_1^T H_1$) can be written as:

$$A^{\#} = \frac{A^T}{A^T A + \bar{p}(\|A\|)}, \tag{21}$$

where $\bar{p}(\|A\|)$ is a bell-shaped, finite support, positive scalar function of the norm of vector A, which is used to prevent $A^{\#}$ from growing unbounded whenever A is close to zero.

Using (20), and under the assumption that no regularization is necessary ($\bar{p} = 0$), the corresponding error rate becomes

$$\dot{\sigma}_1 = \dot{\tilde{\sigma}}_1 \tag{22}$$

because the presence of the orthogonal projector $\left[I - \left(n_1^T H_1\right)^{\#} \left(n_1^T H_1\right) \right]$ projects z_1 on the null subspace of $n_1^T H_1$.

Instead, if $\alpha_1 = 0$, i.e. when the associated inequality objective is achieved, a full arbitrariness in the system velocity vector y is allowed, simply because the cost functional disappears. Indeed, the corresponding manifold of solutions is:

$$y = z_1 \ ; \ \forall z_1. \tag{23}$$

To make a comparison with (20), it can be said that the minimum norm solution is now equal to zero, and that the orthogonal projector is simply the identity matrix. In addition note how in this case the error rate is no more coincident with its reference (as the task is not active) and, it instead, results to be

$$\dot{\sigma}_1 = n_1^T H_1 z_1 \ ; \ \forall z_1, \tag{24}$$

i.e. fully dependent on the selection of z_1 (as it will be evidenced in the next section). Note that this allows to overcome the problem stated in the previous section, i.e. the fact that $\dot{\sigma}_1$ is not forced to be 0 inside the validity region of the inequality constraint.

However, it is clear that the allowed arbitrariness space, represented by the orthogonal projector, exhibits an abrupt discontinuity in the vicinities of $\alpha_1 = 0$, because its dimension changes from N to $N-1$ as α_1 increases from 0. Since the allowed arbitrariness is exploited by the immediately following lower priority task, it is then evident how such a discontinuity is prone to induce chattering phenomena just in the vicinities of $\alpha_1 = 0$.

In order to avoid such a drawback, let us first rewrite (19) in a form that allows to deal with both the above cases $\alpha_1 = 0$ and $\alpha_1 \neq 0$. This can be simply done by putting α_1^2 inside the norm to be minimized, and explicitly carrying out the multiplication with the term $\dot{\bar{\sigma}}_1 - n_1^T H_1 y$, leading to

$$\mathcal{S}_1 \triangleq \left\{ y = \arg\min_y \left\| \alpha_1 \dot{\bar{\sigma}}_1 - \alpha_1 n_1^T H_1 y \right\|^2 \right\}. \tag{25}$$

The manifold of solutions of this problem has a similar expression as in (20), namely

$$y = (\alpha_1 n_1^T H_1)^{\#} \alpha_1 \dot{\bar{\sigma}}_1 + \left[I - (\alpha_1 n_1^T H_1)^{\#} \alpha_1 n_1^T H_1 \right] z_1, \tag{26}$$

which is also comprehensive of the solutions (23) obtained for $\alpha_1 = 0$.

Now the main idea for avoiding the chattering phenomena is using a regularizing function $p(\cdot)$ that, differing from $\bar{p}(\cdot)$ in (21), is now dependent not only on the norm of the product $\alpha_1 n_1^T H_1$, but also explicitly on α_1,

in order to obtain the required smoothness for all the values of α_1. Among the possible choices, the one used in TRIDENT is simply

$$p(\alpha_1, \|\alpha_1 n_1^T H_1\|) \triangleq (1 - \alpha_1) + \bar{p}(\|n_1^T H_1\|). \tag{27}$$

With the use of such regularizing function, the expression of the pseudo inverse in (26) becomes

$$(\alpha_1 n_1^T H_1)^{\#} = \frac{\alpha_1 H_1^T n_1}{\alpha_1^2 n_1^T H_1 H_1^T n_1 + (1 - \alpha_1) + \bar{p}(\|n_1^T H_1\|)}. \tag{28}$$

Now to show that the above equation exhibits a smooth behavior, let us start by assuming that the vector $n_1^T H_1$ is not singular (as previously done). This implies that $\bar{p} = 0$. Then let us define $Q_1 \triangleq \left[I - (\alpha_1 n_1^T H_1)^{\#} \alpha_1 n_1^T H_1\right]$ and let us consider the following three possible cases:

1. if $\alpha_1 = 1$ then $p = 0$ and (28) simply reduces to the standard pseudo inverse of vector $n_1^T H_1$. This implies that Q_1 is an orthogonal projector of rank $N - 1$, and thus that (26) is the same as (20);

2. if $\alpha_1 = 0$ then $(\alpha_1 n_1^T H_1)^{\#} = 0$. As a consequence, Q_1 is the identity matrix of rank N, and (26) is the same as (23);

3. if $0 < \alpha_1 < 1$, the regularization makes $(\alpha_1 n_1^T H_1)^{\#}$ smoothly evolve between the previous two cases, and the same holds for matrix Q_1 (which in this case is no more an orthogonal projector). Furthermore note that the corresponding error rate $\dot{\sigma_1}$ varies from (22) to (24).

As a final remark note that in case the norm of vector $n_1^T H_1$ exhibits a null or quasi-null value (due to a singular posture of the robot), the term $\bar{p}(\cdot)$ in (27) still prevents the pseudo inverse to grow unbounded, as in (21).

Having tackled the problem of smooth activation and deactivation of a single inequality task, let us conclude the present subsection by introducing the following more compact notation, that shall be used in all the successive ones:

$$\dot{\bar{\zeta}}_1 \triangleq \alpha_1 \dot{\bar{\sigma}}_1, \tag{29}$$

$$G_1 \triangleq \alpha_1 n_1^T H_1, \tag{30}$$

$$\rho_1 \triangleq G_1^{\#} \alpha_1 \dot{\bar{\sigma}}_1, \tag{31}$$

$$Q_1 \triangleq \left[I - G_1^{\#} G_1\right]. \tag{32}$$

3.5 Managing Lower Priority Inequality Objectives

Passing to consider the second inequality control objective, to be managed within the arbitrariness space allowed by the first one, we have the following, now linearly constrained, linear quadratic minimization problem

$$\mathcal{S}_2 \triangleq \left\{ y = \arg\min_{y \in \mathcal{S}_1} \left\| \dot{\tilde{\zeta}}_2 - G_2 y \right\|^2 \right\}. \tag{33}$$

By accounting for the constraint (20), the above can be equivalently rewritten as

$$\mathcal{S}_2 \triangleq \left\{ y = \rho_1 + Q_1 z_1 : z_1 = \arg\min_{z_1} \left\| (\dot{\tilde{\zeta}}_2 - G_2 \rho_1) - \hat{G}_2 z_1 \right\|^2 \right\}, \tag{34}$$

where we have preliminarily let

$$\hat{G}_2 \triangleq G_2 Q_1, \tag{35}$$

therefore leading to the following linear manifold of solutions for z_1

$$z_1 = \hat{G}_2^{\#} \left(\dot{\tilde{\zeta}}_2 - G_2 \rho_1 \right) + (I - \hat{G}_2^{\#} \hat{G}_2) z_2 \ \ ; \ \ \forall z_2 \tag{36}$$

and for y

$$\begin{aligned} y &= \left(\rho_1 + Q_1 \hat{G}_2^{\#} \left(\dot{\tilde{\zeta}}_2 - G_2 \rho_1 \right) \right) + Q_1 (I - \hat{G}_2^{\#} \hat{G}_2) z_2 \\ &\triangleq \rho_2 + Q_2 z_2 \ \ ; \ \ \forall z_2 \end{aligned} \tag{37}$$

It is at this point clear how the above process can be further iterated by exploring, in a descending priority order, all successive objectives, thus leading to the following task-priority based algorithmic structure.

With the initialization

$$\rho_0 = 0 \quad ; \quad Q_0 = I \tag{38}$$

then for $i = 1, \ldots, k$, where k is the total number of the former prioritized sequence of inequality tasks:

$$\begin{aligned} \hat{G}_i &\triangleq G_i Q_{i-1} \\ T_i &\triangleq \left(I - Q_{i-1} \hat{G}_i^{\#} G_i \right) \\ \rho_i &= T_i \rho_{i-1} + Q_{i-1} \hat{G}_i^{\#} \dot{\tilde{\zeta}}_i \\ Q_i &= Q_{i-1} (I - \hat{G}_i^{\#} \hat{G}_i) \end{aligned} \tag{39}$$

thus ending up with the final control law

$$y = \rho_k + Q_k z_k \ \ ; \ \ \forall z_k, \tag{40}$$

where the residual arbitrariness $Q_k z_k$ has to be used for managing the remaining equality type control objectives, as indicated in the following subsection.

3.6 Managing Lower Priority Equality Objectives

By now restarting at the $k+1$ priority level, where the highest priority equality task is located, we now encounter the following linearly constrained linear quadratic minimization problem

$$\mathcal{S}_{k+1} \triangleq \left\{ y = \arg\min_{y \in \mathcal{S}_k} \left\| \dot{\bar{\zeta}}_{k+1} - G_{k+1} y \right\|^2 \right\}, \tag{41}$$

which is formally identical to the ones for inequality objectives, apart from the fact that, being now $\alpha_{k+1} \equiv 1$ (as it is also for all other remaining equality tasks) we now have

$$\begin{aligned} \dot{\bar{\zeta}}_{k+1} &\triangleq \dot{\bar{\sigma}}_{k+1}, \\ G_{k+1} &\triangleq n_{k+1}^T H_{k+1}. \end{aligned} \tag{42}$$

Unfortunately, in case the considered equality objective requires the zeroing of its relevant error (as it is within the TRIDENT system, for both its two equality objectives regarding the end-effector approach), it occurs that in the vicinity of the error vector zeroing, the corresponding unit vector n_{k+1} tends to become ill defined. If no counter measures are taken, a set of uncontrolled phenomena, as for example chattering around $\sigma_{k+1} = 0$, are almost sure to occur.

In order to avoid such inconvenience, a simple counter measure exists, consisting of substituting the use of the above scalar and row-vector quantities (42) with the following ones

$$\begin{aligned} \dot{\bar{\zeta}}_{k+1} &\triangleq \dot{\bar{s}}_{k+1} = -\gamma s \\ G_{k+1} &\triangleq H_{k+1}, \end{aligned} \tag{43}$$

where the error reference vector $\dot{\bar{s}}_{k+1}$ can be directly evaluated without needing its unit vector. Furthermore, the unit vector n_{k+1} does not appear anymore in the Jacobian matrix G_{k+1}. However, as it can be easily seen, the cost to be paid when using (43) in lieu of (42) is that this may require the engagement of up to

three degrees of mobility (provided they are available at the current stage) instead of a single one, as it is for inequality objectives, or for the equality ones not requiring their error zeroing.

The use of the above correction directly extends to all the remaining equality objectives, allowing one to complete the previous algorithmic recursion (39) for inequality objectives with a structurally identical one, only differing in the substitutions (42), (43) when necessary.

The resulting global algorithm now extends to the final L-th objective, leading to the final value for the control action

$$y = \rho_L, \tag{44}$$

where the eventual arbitrariness still left has to be set to zero since it is not necessary anymore for the given list of prioritized control objectives.

Finally also note how the obtained global algorithm is (as it could not be otherwise) independent from the control objective ordering. This implies that it could be used also for cases where, for some reasons, inequality and equality objectives were not ordered as instead it has been explicitly suggested for the TRIDENT system.

3.7 Subsystem Priorities

In case the above devised prioritized control procedure is applied to the TRIDENT system, no priority subsystem motions can actually emerge. This is due to the fact that the overall system velocity vector y is employed without any prioritized distinction between its composing parts.

As a consequence of this both the arm and vehicle will be generally moving, even when not strictly necessary. For instance, with the approach of the previous section, this happens when the end-effector is sufficiently close to the object to be grasped, in such a way that the sole arm motion would be enough, without the need of involving the vehicle. Generally, in these conditions, moving the vehicle as little as possible is instead very advisable, especially in cases where the mass and inertia of the vehicle are sensibly higher than those of the arm; and this not only for energy saving reasons, but also because the vehicle motions are typically much less precise than the arm ones. However, such inconvenience might be avoided by including, as the $(L+1)$-th additional task with least priority, the following

$$\mathcal{S}_{L+1} \triangleq \left\{ y = \arg \min_{y \in \mathcal{S}_L} \|v\|^2 \right\}, \tag{45}$$

which would always constrain the vehicle motions to solely be the strictly necessary ones.

4 Task-priority and Dynamic Programming Based Coordinated Control for Floating Manipulation

In this section we shall present the already announced task-priority and DP based control procedure that, other than being intrinsically inclusive of subsystem motion priorities, also introduces non negligible benefits when dealing with multi-rate situations (as it is for the TRIDENT vehicle and arm which are controlled at 10 Hz and 100 Hz, respectively) and/or when a possible velocity disturbance (as for instance sea currents, even of non stationary type) is superimposed on the vehicle one.

4.1 General Idea of the Dynamic Programming Approach

The DP based approach develops by first of all subdividing the overall kinematic chain into composing subchains. Then a "backward direction of exploration" of the resulting sequence of subchains is chosen.

By following the chosen exploration path, the sequence of prioritized tasks is processed for the first subchain, by letting the velocities of the underlying ones be the given parameters at the current sampling instant. The resulting control law for the first subchain is consequently obtained, parametrized by the velocities of its underlying ones.

Then the same procedure is sequentially repeated in correspondence of each one of the so backward encountered subchains, even if now with the addition of the conditioning provided by the control law devised of the upper-lying subchain. For each subchain, a parametrized control law is consequently obtained, which accounts for the one relevant to its corresponding upper-lying one.

4.2 Dynamic Programming Applied to TRIDENT

When applied to the TRIDENT system, the DP based procedure naturally suggests the arm as the starting subchain. In this way, by requiring the arm to be the first subchain in maximally exploiting its degrees of mobility for gathering all prioritized tasks (only those involving joint velocities will be gathered by the arm) the vehicle will be then naturally required to move only for achieving its own objectives (i.e. camera centering, etc.), if any to be achieved. However, the vehicle can still help the arm for any objective also

involving the vehicle velocity (explicitly or implicitly, via the arm control law itself), when necessary. In any case, this procedure naturally implies a minimality of motion by part of the vehicle in any condition.

So, within the TRIDENT system, by starting with the arm, the following sequence of minimizations must be performed

$$\mathcal{S}_i = \left\{ \dot{q} = \arg \min_{\dot{q} \in S_{i-1}} \left\| \left[\dot{\bar{\zeta}}_i - G_i^v v \right] - G_i^a \dot{q} \right\|^2 / v \right\}, \tag{46}$$

where the overall contribution $G_i y$, defined as (29) for inequalities or (43) for equalities, has been now split into $G_i^v v$ and $G_i^a \dot{q}$, i.e. into the contributions separately provided by the vehicle and the arm, respectively. Furthermore, note how the part in brackets plays the role of an equivalent, parametrized by v, reference signal.

Then, following steps strictly identical to those already shown in Section 3.5, after the initializations

$$\bar{\rho}_0 = 0 \;\; ; \;\; Q_0 = I \;\; ; \;\; P_0 = 0 \tag{47}$$

the following recursive formulation is obtained (where the additional presence of the matrix P_i naturally arises within the minimization process just for taking into account of the influence of the vehicle velocity via superposition, that is as the sum of the contributions provided by its components, when interpreted as separately acting)

$$\begin{aligned} \hat{G}_i^a &\triangleq G_i^a Q_{i-1} \\ T_i &\triangleq \left(I - Q_{i-1} (\hat{G}_i^a)^{\#} G_i^a \right) \\ P_i &= T_i P_{i-1} - Q_{i-1} (\hat{G}_i^a)^{\#} G_i^v \\ \bar{\rho}_i &= T_i \bar{\rho}_{i-1} + Q_{i-1} (\hat{G}_i^a)^{\#} \dot{\bar{\zeta}}_i \\ Q_i &= Q_{i-1} \left(I - (\hat{G}_i^a)^{\#} \hat{G}_i^a \right) \end{aligned} \tag{48}$$

thus ending with the final parameterized control law for the arm

$$\dot{\bar{q}} = \dot{q}(\bar{\rho}^a, v) = \bar{\rho}^a + P v, \tag{49}$$

where $\bar{\rho}^a$ is the final value attained by vector $\bar{\rho}_i$ in the above recursion, and where any eventual arbitrariness still left in the joint velocities has to be set to zero, since it is not necessary anymore, at arm level, for the now completed list of prioritized control objectives.

The successive minimizations will still regard the same list of prioritized objectives, but now performed with

respect to the vehicle velocity parameter, with conditioning provided by the above devised parametrized control law for the arm, as hereafter described

$$\mathcal{S}_i \triangleq \left\{ v = \arg \min_{v \in S_{i-1}} \left\| \left[\dot{\bar{\zeta}}_i - G_i^v v \right] - G_i^a \dot{q} \right\|^2 / \dot{q}(\bar{\rho}^a, v) \right\}. \tag{50}$$

By substituting the arm control law (49) in lieu of $\dot{q}$, the following equivalent representation is then obtained

$$\mathcal{S}_i \triangleq \left\{ v = \arg \min_{v \in S_{i-1}} \left\| \left(\dot{\bar{\zeta}}_i - G_i^a \bar{\rho}^a \right) - F_i v \right\|^2 \right\}, \tag{51}$$

where $F_i \triangleq (G_i^v + G_i^a P)$. Then, since (51) is it also structurally the same as (46), after the initializations

$$\bar{\rho}_0 = 0 \;\; ; \;\; Q_0 = I \tag{52}$$

the following set of equations can be therefore found, for $i = 1, \ldots, L$

$$\begin{aligned} \hat{F}_i &\triangleq F_i Q_{i-1} \\ T_i &= \left(I - Q_{i-1} \hat{F}_i^{\#} F_i \right) \\ \bar{\rho}_i &= T_i \bar{\rho}_{i-1} + Q_{i-1} \hat{F}_i^{\#} \left(\dot{\bar{\zeta}}_i - G_i^a \bar{\rho}^a \right) \\ Q_i &= Q_{i-1} \left(I - \hat{F}_i^{\#} \hat{F}_i \right) \end{aligned} \tag{53}$$

thus now ending with the following control action for the vehicle

$$\bar{v} = \bar{\rho}^v, \tag{54}$$

where $\bar{\rho}^v$ is the final value attained by vector $\bar{\rho}_i$ in the above recursion for the vehicle. Again, any eventual arbitrariness still left has to be set to zero, since it is not necessary anymore for the (now totally completed) list of prioritized control objectives. Since the above is actually a control action, it can be finally substituted into the control law (49) for the arm, in order to get the corresponding control action.

4.3 Compensation of Disturbances

Following the results of the above section, the implementation of the successive forward phase of the DP thus reduces to the following simple substitution

$$\bar{y} = \begin{cases} \dot{\bar{q}} = \dot{q}(\bar{\rho}^a, v) = \bar{\rho}^a + P\bar{\rho}^v \\ \bar{v} = \bar{\rho}^v \end{cases} . \tag{55}$$

Generally, the choice of explicitly performing the above substitution is *not* the most convenient one, since it prevents the exploitation of another important peculiar property exhibited by the DP approach: the more efficient management of vehicle velocity disturbances and/or vehicle velocity inaccuracies, that could be exhibited at vehicle level.

In order to be more precise, note how the arm-level control law is the best one to be employed in correspondence of *any* velocity v exhibited by the underlying vehicle (and the successive definition of a suitable $\bar{v}$ for the vehicle just serves for further improving what the arm is already per-se performing at best).

Then, by explicitly taking into account this property, the arm kinematic controller should preferably use the actual vehicle velocity v as one of its inputs, in lieu of the computed one $\bar{v}$, which is in any case commanded to the vehicle; thus automatically compensating for the mentioned possible vehicle velocity tracking inaccuracies and/or velocity disturbances occurring at the vehicle level.

The possibility of compensating for vehicle velocity perturbations directly arises as a specific property exhibited by the DP approach, which cannot be easily identified within the standard one.

4.4 Multi-rate Sampling

In case of multi-rate sampling, as it is for TRIDENT, where the arm is controlled at 100 Hz and the vehicle at 10 Hz, it is sufficient to consider the larger period of 0.1s subdivided into 10 sub-periods of 0.01s, and then notice how, during the first subperiod, the DP procedure will have to run entirely along the two subchains (i.e. arm and vehicle). Both the joint and vehicle velocity reference $\dot{\bar{q}}$, $\bar{v}$ will be computed for the first subperiod, while the latter ones will be held as a constant vehicle velocity reference for all the remaining nine subperiods.

During each one of the remaining nine subperiods, the kinematic controller will therefore have to limit itself

to run the DP part relevant to the arm level only, while using $\bar{v}$ (or the actual vehicle velocity v if available) as a constant parameter.

Here also we can note how the evidenced capability of easily handling multi-rate sampling situations, as indicated above, it also emerges as a peculiar property exhibited by the DP approach.

4.5 Adopted Task Scheduling

The adopted detailed descending priority ordering of the various objectives has been assigned by following this order for the arm: arm joint limits, arm manipulability, arm elbow angle, linear end-effector approach, angular end-effector approach. The reason for this choice is simple. Joint limits are the most important inequality constraints that the arm has to satisfy, since they are related to the safety of the system itself. Violating such bounds would mean that some joint has reached its own physical limit (with the risk of damaging itself) and thus cannot move further. After this task, the manipulability has been chosen next. This task is instead operational-enabling, since it maintains a good dexterity of the arm, preventing it from reaching singular postures. The arm elbow angle task is also operational-enabling, since it avoids unnecessary occlusions between the camera and the object to be grasped, which could be caused by the arm elbow movements. Finally, the two equality tasks related to the end-effector positioning are found.

The list of tasks for the vehicle is the following: arm joint limits, camera distance, camera height, camera centering, arm manipulability, arm elbow angle, linear end-effector approach, angular end-effector approach. Again, note that the only task related to the safety of the system is listed as first. Then, the trio of tasks related to the object pose estimate, i.e. camera distance, height and centering are present. They are operational-enabling tasks, since without them there would be no constraint to keep the object within the camera field of view. Finally, following the same priority for the arm and with the same rationale, the manipulability, arm elbow angle and the equality end-effector tasks are found.

5 TRIDENT Overall Control Architecture

The previously developed task priority based control procedure solely represents the so-called Kinematic Control Layer (KCL) of the overall control architecture. Such a layer is the one in charge of real-time generating the system velocity vector $\bar{y}$ as a reference one, which is then real-time tracked by an appropriate underlying Dynamic Control Layer (DCL), acting at the level of vehicle thrusters τ and arm joint torques

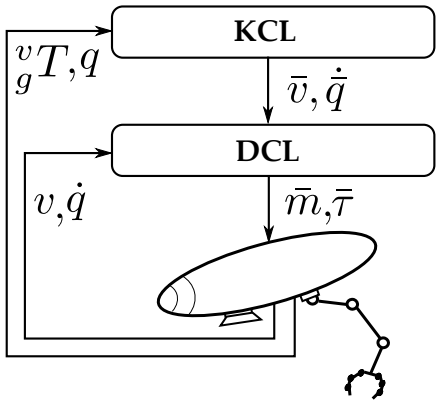

Figure 4: TRIDENT's two layered architecture: the KCL generates the references for the underlying DCL using the proposed task-priority approach

m, accordingly to what appears sketched in Fig. 4.

This type of control architecture extends the one that within the robotic literature in generally termed as back-stepping approach (see for instance [Aicardi et al., 1995]) to robot control to the case of prioritized inequality and equality objective.

A detailed structuring and analysis of the DCL can be found in the preliminary work [Casalino, 2011], which also covers the cases of very rough dynamic model approximation. Remarkably within such work it is also shown how the Dynamic Programming procedure also applies to the DCL with the same philosophy (upon a suitable reformulation of the system dynamic model). This induces advantages strictly similar to the ones obtained for KLC, in particular an improved capability of now compensating, at DCL level, for vehicle thrusters force/torque generation mismatches.

Furthermore, this approach can be easily applied when the subsystems have their own lower level controller already developed, and/or the force/torque commands are not available, as it has been the case in TRIDENT.

Instead, other approaches to robot control (potentially more efficient, even if generally more computationally expensive) start by directly dealing with a dynamic model of the robot suitably projected in the operational space (to this respect see for instance the seminal work [Khatib, 1987] or [Siciliano et al., 2009]). However, it is the opinion of the authors that such approaches are still far from also efficiently allowing the management of prioritized multi-objective situations, as it instead clearly happens within the here adopted back-stepping approach. Indeed, operational space based dynamic approaches still generally deal with single-objective situations, typically the sole end-effector reaching problem.

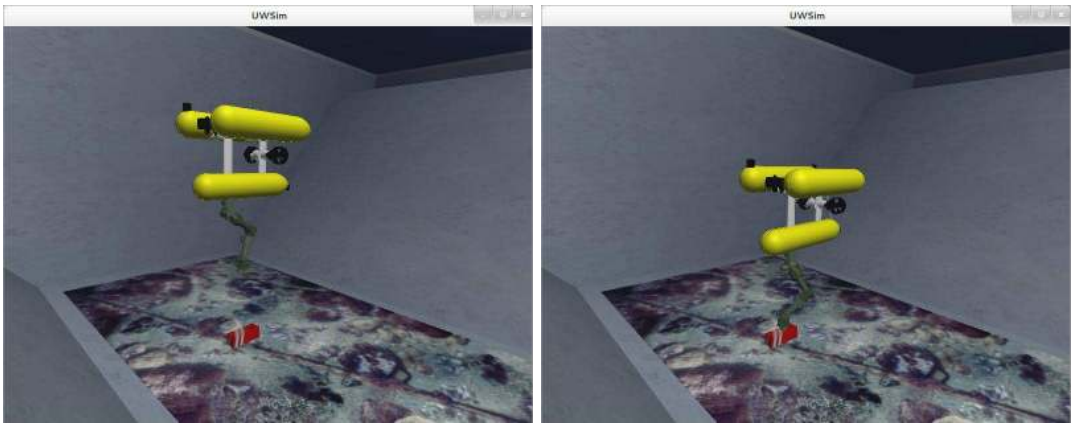

(a) (b)

Figure 5: Simulation trial: (a) starting position (t = 0s) (b) final position (t = 60s)

6 Simulation Trials

In this section, for the sake of brevity only one simulation result will be presented, demonstrating the effectiveness of the proposed coordinated control architecture. Other simulations can be found in [Casalino et al., 2012a, Casalino et al., 2012b].

In the simulation environment depicted in Fig. 5(a), the object is located at $[2.5m\ 2m\ 4.75m]$ with respect to a world frame with z axis going towards the depth of the pool. The vehicle initial position is $[2.15m\ 1m\ 3m]$, which is about on top of the object, with it grossly inside the field of view of the vision system, placed on the vehicle near the base of the arm. The vehicle, other than providing all three linear velocities, is only actuated on the yaw, thus providing 4 d.o.f., while roll and pitch are assumed passively stable. This explains why the horizontal attitude task has not been included in the task list.

Figure 6 shows the time history of the $\alpha_{(\cdot)}$ functions, as defined in (19), where the subscript refers to the error-vector directly related to the corresponding task (see subsection 3.2 for their definition).

As can be seen, the system starts in a configuration where the manipulability is good ($\alpha_\mu = 0$), and proceeds to perform a better centering of the object. Whilst doing so, the arm is also trying to reach the object for the grasp. This requires a movement of the arm in the z plane, tending to induce a loss of manipulability, which is however countered by the overall system, since the corresponding α_μ becomes $\neq 0$ but never reaches 1. The same is valid for the joint limit of the joint number 4, as can be appreciated by the history of the corresponding α function in the right-side picture of Fig. 6. The system also avoids occlusions of the elbow of the arm with the vision system, by keeping the corresponding α_ψ below 1.

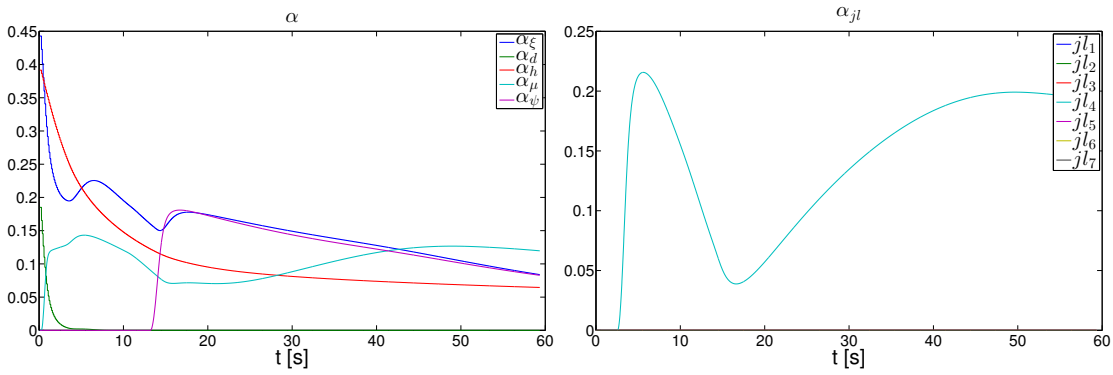

(a) (b)

Figure 6: Simulation trial: time history of the α functions (a) camera centering, camera distance, camera height, manipulability and arm elbow tasks (b) joint limits task

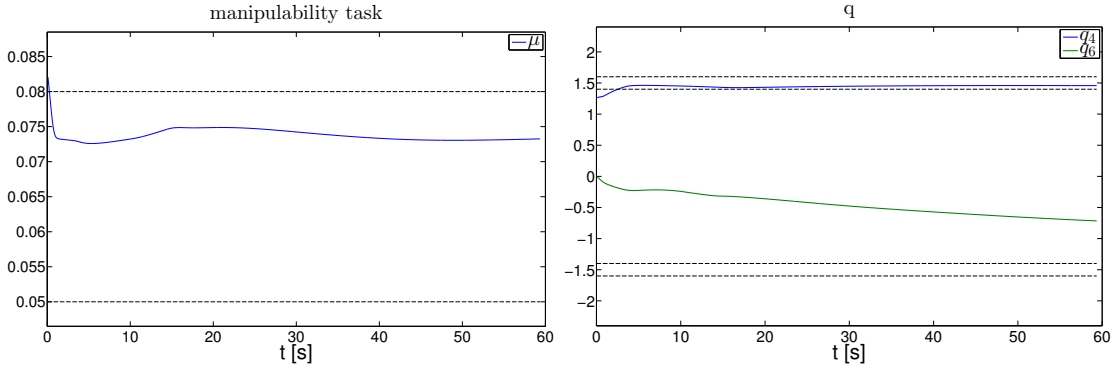

(a) (b)

Figure 7: Simulation trial: (a) time history of the manipulability measure μ (b) time history of the q vector

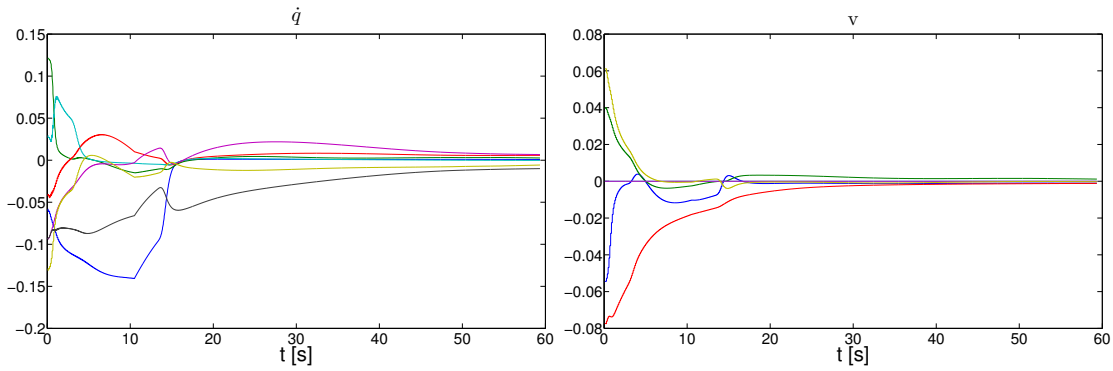

(a) (b)

Figure 8: Simulation trial: (a) time history of joint velocity vector $\dot{q}$ (b) time history of the vehicle velocity vector v

Figures 7(a) and 7(b) show the history of the manipulability measure μ and the history of the q vector. As it can be seen, the manipulability is maintained within the required thresholds, which in these specific examples are $\mu > 0.05$, and the corresponding α_μ function begins to activate when $\mu < 0.08$. This guarantees that the manipulability measure never falls below $\mu = 0.05$.

A similar example can be seen when looking at the q vector. The q_4 goes near its own physical bound, causing the activation of the corresponding joint limit task. This task maintains the q_4 from further approaching its physical limit, as can be appreciated in Fig. 7(b). Other joints, like for example q_6, since they are far away from their own limit, do not have their corresponding α value active, and thus are freely used by the system.

Finally, Fig. 8(a) reports the time history of the joint velocity vector $\dot{q}$, while Fig. 8(b) instead shows the history of the vehicle velocity, highlighting the continuity of the proposed approach. The small jumps in the required velocities for the arm are due to the multi-rate nature of the control, since the vehicle position is only updated at a slower rate (10Hz feedback versus a control rate for the arm of 100Hz) and thus creating small jumps also in all the references that are depending on the sensor feedback.

7 Experimental Trials

In this section, two different experimental trials will be presented. The first trial was carried out in the water tank of the Centre d'Investigació en Robòtica Submarina - CIRS of the University of Girona. The second trial was instead carried out in Port Sòller, Majorca, in a retired Naval base harbor.

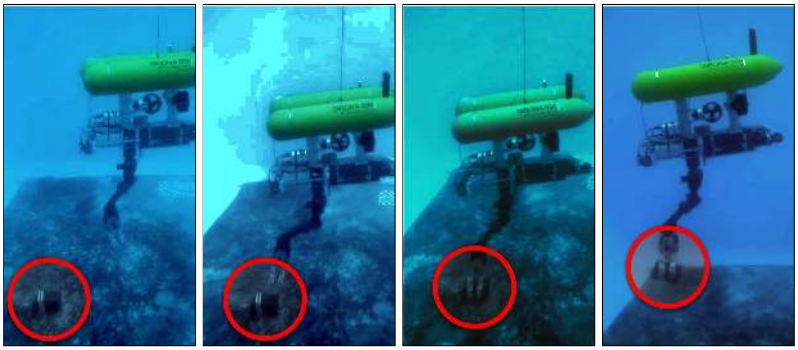

(a) (b) (c) (d)

Figure 9: Experimental trial in Girona pool: snapshots of the movement of the I-AUV. The red circle highlights the position of the black box to be retrieved

7.1 From Theory to Practice

Before presenting the experimental results, let us first comment the transition from the theoretical to the actual implementation. Preliminary trials showed the need of an additional task to prevent the occlusions between the object and the camera frame caused by the arm elbow. Due to the modularity of the proposed approach, introducing such a new task was quite easy, even from the software point of view, as it required just one more recursion of the algorithm (48), (53).

Further changes were needed for the control gains and the thresholds for the activation and deactivation of the sigmoid functions α. To this respect, a fundamental role was played by how the software was designed and structured. Indeed, all the control parameters such as gains, thresholds, and so on were changeable in real-time with the use of a remote graphical interface, without the need of recompiling the software. This allowed to greatly reduce the time from trial to trial. Furthermore, the activation of each task could be tracked in real-time in the GUI, so it was quite easy to detect problems, as for example conflicts between tasks due to badly chosen boundaries for the α functions. Finally, all the data was logged to be post-processed and analyzed.

7.2 Pool Trials

The testing and the integration of the algorithms has been carried out mainly at the CIRS pool in Girona, Spain. In this section, one of the experiments and its results are presented. Figure 9 shows a few snapshots of the I-AUV performing the free-floating manipulation, and successfully recovering the object from the floor of the pool. As it can be noticed, the floor is covered by a print representing a possible seafloor image.

The vision system was running at just 2Hz. This can be appreciated in some graphs, like for example in Fig. 10, where the time history of the activation functions is reported. The multi-rate nature of the data and the control can be easily noticed.

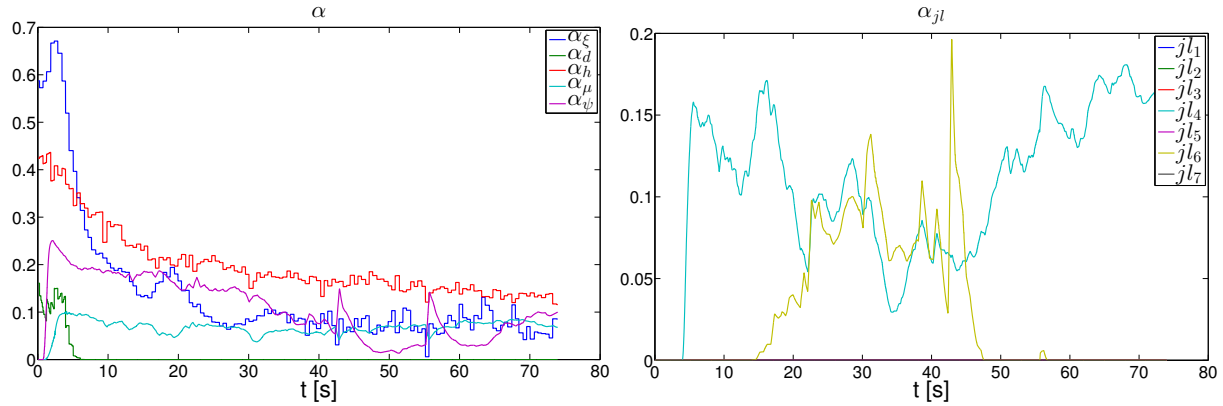

(a) (b)

Figure 10: Girona pool trials: time history of the α functions of the inequality tasks

The Fig. 10(a) shows how many of the inequality tasks were active during the trial: camera centering and camera height tasks were active for the duration of the free floating control; the manipulability and the elbow occlusion tasks quickly became active and remained so; the camera distance instead started as active but became inactive after a few seconds. Figure 10(b) shows instead that during the trial two joints (number 4 and 6) were close to their physical limit.

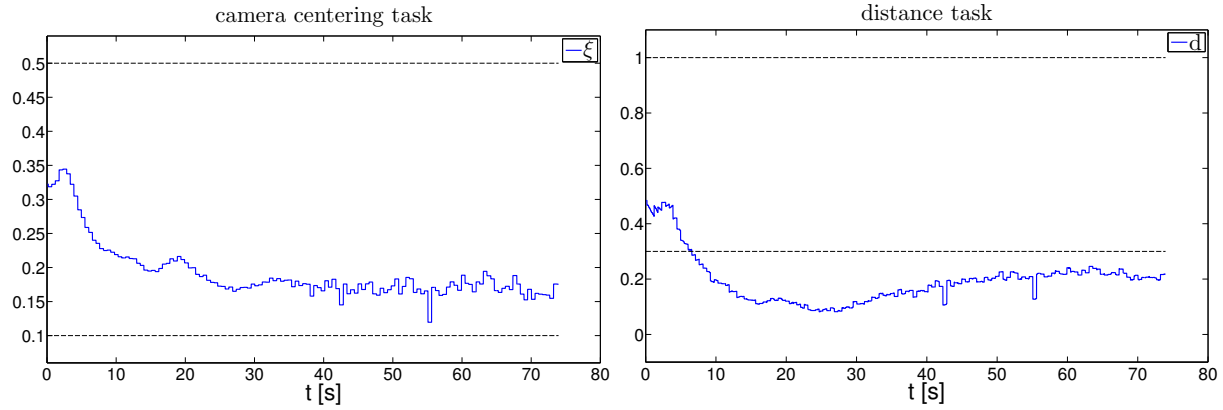

(a) (b)

Figure 11: Girona pool trials: time history of (a) camera centering errors (b) camera distance errors

Figure 11(a) shows how the camera centering error was always between the two bounds of the activation function, thus the corresponding α was always between 0 and 1. Instead, Fig. 11(b) reports how the camera distance task error went under the activation bound after about 10s, deactivating the task.

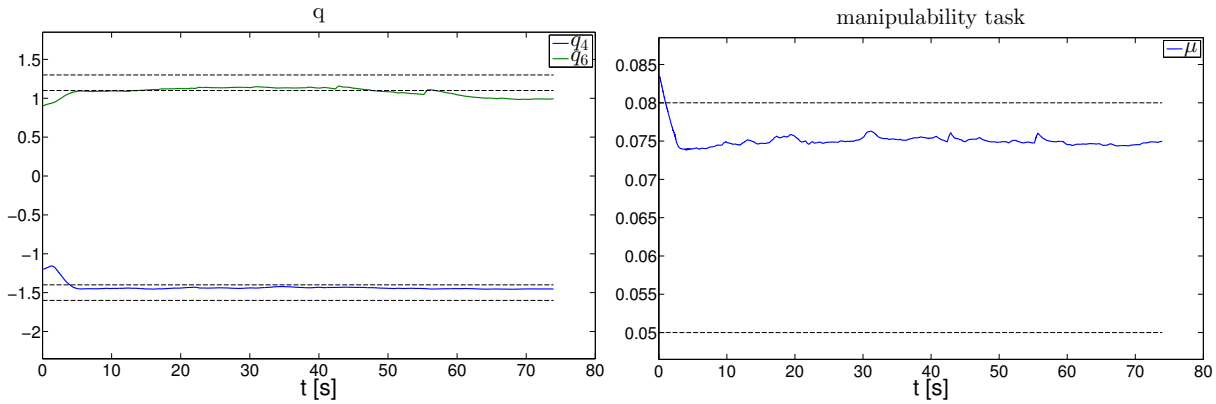

(a) (b)

Figure 12: Girona pool trials: time history of (a) q positions near end of races (b) manipulability measure

The successive Fig. 12 depicts the arm related tasks. In the first Fig. 12(a) it can be appreciated how the joints near their physical limit never violate them. The second Fig. 12(b) shows instead how the system manages to stop the decrease of the manipulability measure (thus keeping a good arm dexterity) once inside the higher bound. The initial decrease of manipulability is due to the fact that the arm is trying to reach the object for the grasp, thus stretching forward and losing dexterity.

7.3 Sea Trials

The first field experiments were carried out during the first week of October 2012, inside the Port Sòller navy harbor on the island of Majorca. Due to low number of features on the terrain, the vision algorithm could not work properly when occluded by the hand (i.e. when grasping the box), so it had to be substituted by the integration of the vehicle's odometry (DVL for linear velocity and gyroscopes for angular velocity) whenever an occlusion was detected. This was a major difference w.r.t. the pool trials, since the print covering the floor of the water tank had many features and the pose estimation algorithm could easily continue to work even with occlusions of the black box. From the point of view of the presented work nothing changes, because the pose estimation is an input to the whole algorithm, and a deep discussion of target tracking techniques employed within TRIDENT is out of scope of this work. It is however clear that substituting the pose estimation with odometry integration means that the system is going open-loop, which is clearly a less than ideal situation. However, since the occlusions were occurring only during the very last phases of the grasp, these situations were very limited in time. With this respect, an important part was played by the arm elbow occlusion task, which has prevented the arm from occluding the camera before the final phases of the grasp.

Figure 13 shows some pictures taken from the on-board camera and depicts the phases of the floating manipulation until the successful grasp. As a reference, the black box mock-up was about of 40cm length x 15cm width x 13cm height.

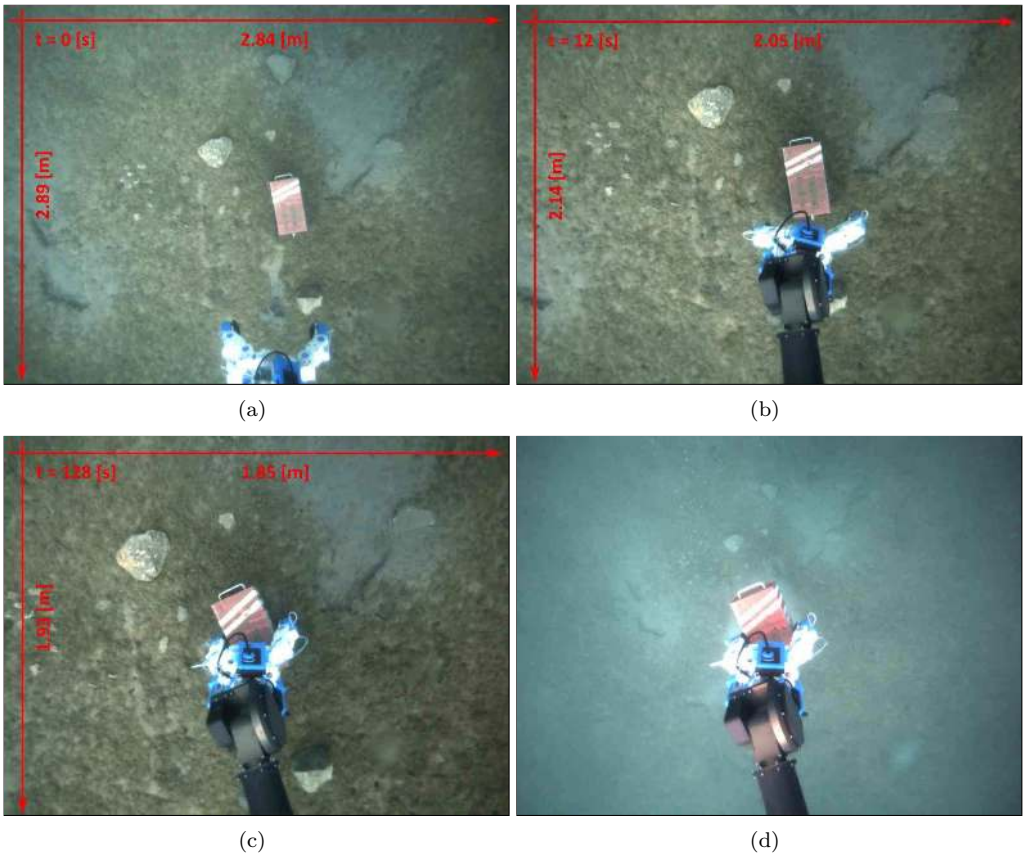

(a) (b)

(c) (d)

Figure 13: Experimental trial in Majorca harbour: snapshots taken from the on-board camera. The approximated extension of the seabed is reported in each frame, along with the time instant

Figure 14 reports the time history of the activation functions, showing how the camera centering and camera height tasks were briefly active at the start of the trial, while the manipulability task was basically always active, preventing the arm from stretching too much and losing dexterity. The figure also shows how one joint was near its physical limit, but the system prevented it from violating such a bound.

Fig. 15(a) shows the commanded $\dot{q}$ for the whole period of the test. Figure 15(b) represents a zoom-in of the first five seconds, highlighting the fact that $\dot{q}$ is continuous. The "step" changes are due to the relatively slow updates (2Hz) coming from the vision system.

Finally, Fig. 16 plots the commanded velocity and the feedback for the vehicle's linear speed. In particular, it is important to notice how the proposed DP approach allows to have an optimal law for the arm even when the vehicle is not following the commanded velocity exactly, as can be clearly seen by Fig. 16.

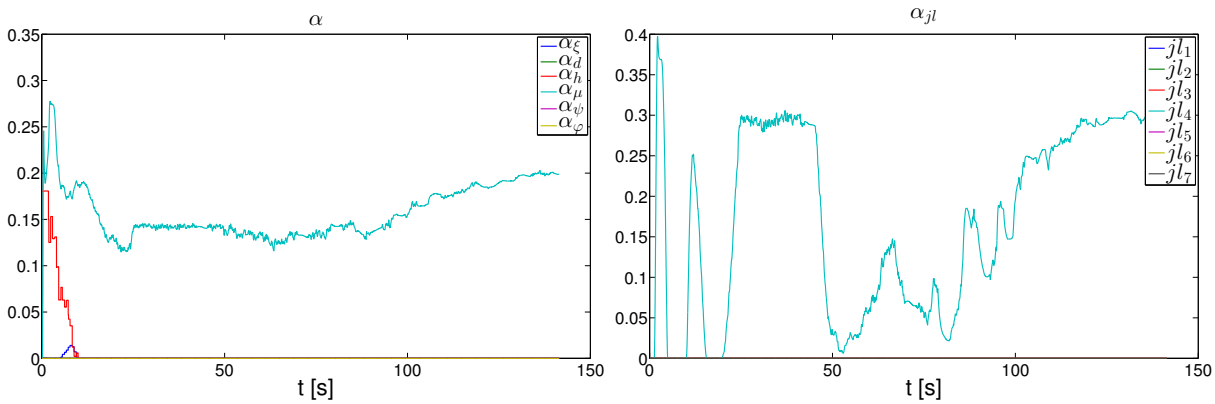

(a) (b)

Figure 14: Majorca harbour trials: time history of the α functions of the inequality tasks

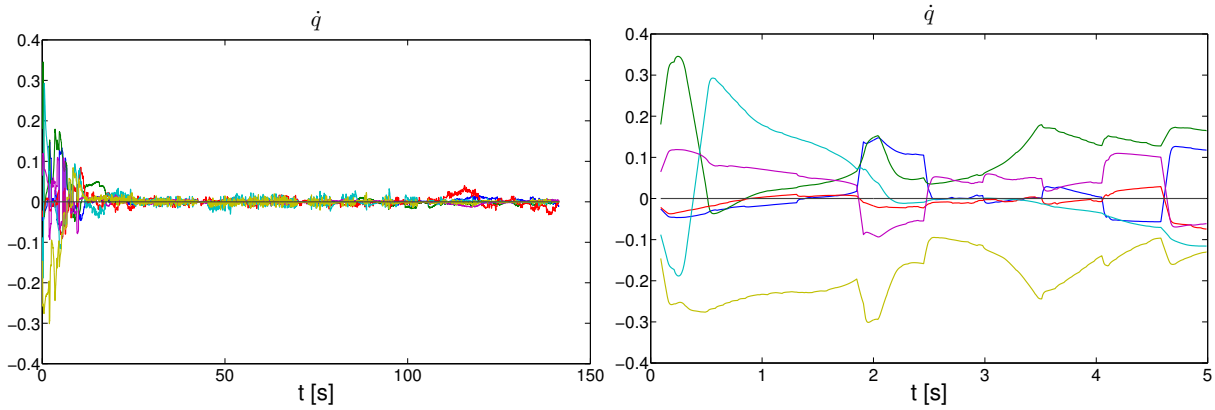

(a) (b)

Figure 15: Majorca harbour trials: time history of the arm velocity reference $\dot{q}$: (a) complete graph (b) zoom to show the continuity

8 Conclusions and Future Works

This paper has presented the overall framework for the coordinated control of the floating manipulation employed within the TRIDENT project. Based on the well known task priority paradigm, the proposed approach extends the original framework by encompassing also scalar inequality constraints, with the use of the so called "activation functions" and the use of a specific algorithmic regularization.

Furthermore, the proposed approach exploits a DP technique, made run between the arm and vehicle sub-chains, which allows to improve the disturbance rejection, since the resulting arm law is optimal w.r.t. any vehicle velocity. A second advantage of the proposed solution is clearly seen in TRIDENT, since the two controls are running at different rates. With the separation created by the DP approach, the multi-rate control is easily tackled. Indeed, the arm control law is computed at a faster rate, using the vehicle feedback

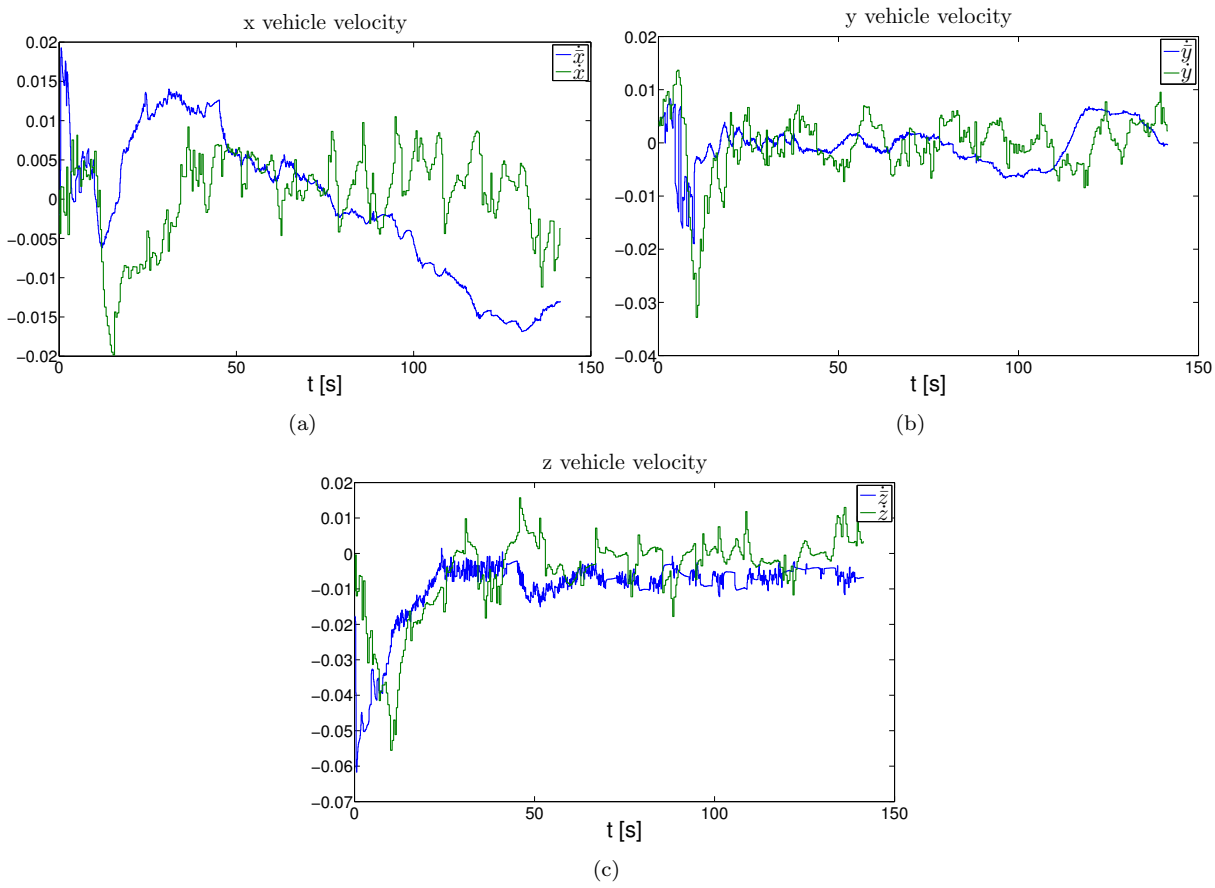

Figure 16: Majorca harbour trials: time history of the vehicle velocity reference v: (a) x velocity command and feedback (b) y velocity command and feedback (c) z velocity command and feedback

whenever available, or the vehicle commanded velocity otherwise.

A simulation example highlighted the continuity of the solution w.r.t. the activation and deactivation of different inequality tasks. Finally two experimental trials have been presented, showing the results obtained with the proposed approach in real scenarios. The first trial is the preliminary experiment carried out in the CIRS pool at University of Girona. In the trial, the system was able to satisfy all the safety constraints, such as joint limits, and recovering the black box from the bottom of the pool. The vision system was running at 2Hz and was also able to continue working with occlusions, due to the picture on the floor of the pool, which contained enough features to continue the pose estimation.

In the sea trial, as evidenced by the pictures taken from the on-board camera, the seafloor was mostly muddy, thus the vision system could not continue to perform the pose estimation whenever an occlusion between the arm-hand system and the box was detected. Even if a specific task to keep the elbow of the arm away from the vision system was active and proved to be working, such occlusions were unavoidable during the final

phases of the grasp, when the hand had to be on top of the box to perform the grasp. In such a situation, the vision feedback was replaced by the odometry of the vehicle, suitably integrated to obtain the position of the object. With this change, the algorithm proved to work well, and enabled the overall system to achieve its final goal and retrieve the box from the sea bottom. This happened even in the presence of sensible differences between the commanded and the actual vehicle velocities, as highlighted by Fig. 16.

Note that the presented work only dealt with the kinematic layer of the free floating control. In TRIDENT, the overall control was separated in two layers, a kinematic and a dynamic one, following the architecture proposed in [Aicardi et al., 1995]. Although the control theory for the dynamic control was fully developed during the TRIDENT project, and is thoroughly reported in [Casalino, 2011], it was not implemented due to timing constraints and the fact that the sole kinematic layer proved sufficient during the preliminary trials in the Girona pool.

Current and future works are aimed at the extension of the proposed technique to multi-dimensional inequality tasks, which were not present in TRIDENT, with the exception of the joint limits tasks, where each row was however decoupled from the others. Further work will concern the dual arm free floating control, and the even more challenging cooperative control of two I-AUVs for the transportation of large objects. In addition, the implementation of the dynamic control developed within TRIDENT will be the focus of future works, in order to also increase the speed of operations of the overall system.

Acknowledgments

This work has been supported by the European Commission through FP7-ICT2009-248497 TRIDENT project and partially by the MIUR through the MARIS prot. 2010FBLHRJ project for the latest systematizations. The authors would like to thank the rest of the TRIDENT consortium for all their work during the project. They also want to thank the reviewers for all the suggestions.

References

Aicardi, M., Caiti, A., Cannata, G., and Casalino, G. (1995). Stability and robustness analysis of a two layered hierarchical architecture for the closed loop control of robots in the operational space. In *Robotics and Automation, 1995. Proceedings., 1995 IEEE International Conference on*, volume 3, pages 2771–2778, Nagoya, Japan. IEEE.

Aikenhead, B. A., Daniell, R. G., and Davis, F. M. (1983). Canadarm and the space shuttle. *Journal of*

Vacuum Science & Technology A: Vacuum, Surfaces, and Films, 1(2):126–132.

Albus, J., Lumia, R., and McCain, H. (1988). Hierarchical control of intelligent machines applied to space station telerobots. *Aerospace and Electronic Systems, IEEE Transactions on*, 24(5):535–541.

Albus, J. S., McCain, H. G., and Lumia, R. (1989). *NASA/NBS standard reference model for telerobot control system architecture (NASREM)*. National Institute of Standards and Technology Gaithersburg, MD.

Andary, J. and Spidaliere, P. (1993). The development test flight of the flight telerobotic servicer: design description and lessons learned. *Robotics and Automation, IEEE Transactions on*, 9(5):664–674.

Antonelli, G. and Chiaverini, S. (1998). Task-priority redundancy resolution for underwater vehicle-manipulator systems. In *Proc. IEEE International Conference on Robotics and Automation*, volume 1, pages 768–773, Leuven, Belgium.

Antonelli, G. and Chiaverini, S. (2003). Fuzzy redundancy resolution and motion coordination for underwater vehicle-manipulator systems. *IEEE Trans. on Fuzzy Systems*, 11(1):109–120.

Ben-Israel, A. and Greville, T. (2003). *Generalized inverses: theory and applications*, volume 15. Springer Verlag.

Casalino, G. (2011). TRIDENT overall system modelling, including all variables needed for reactive coordination. Technical report, ISME. Available online at: http://www.graal.dist.unige.it/files/89.

Casalino, G. and Turetta, A. (2003). Coordination and control of multiarm, non-holonomic mobile manipulators. In *Proc. IEEE/RSJ International Conference on Intelligent Robots and Systems (IROS 2003)*, volume 3, pages 2203–2210, Las Vegas, NV, USA. IEEE.

Casalino, G., Turetta, A., Sorbara, A., and Simetti, E. (2009). Self-organizing control of reconfigurable manipulators: a distributed dynamic programming based approach. In *ASME/IFToMM International Conference on Reconfigurable Mechanisms and Robots (ReMAR 2009)*, pages 632–640, London, UK.

Casalino, G., Zereik, E., Simetti, E., Torelli, S., Sperindé, A., and Turetta, A. (2012a). Agility for underwater floating manipulation task and subsystem priority based control strategy. In *International Conference on Intelligent Robots and Systems (IROS 2012)*, pages 1772–1779, Vilamoura, Portugal.

Casalino, G., Zereik, E., Simetti, E., Torelli, S., Sperindé, A., and Turetta, A. (2012b). A task and subsystem priority based control strategy for underwater floating manipulators. In *IFAC Workshop on Navigation, Guidance and Control of Underwater Vehicles (NGCUV 2012)*, pages 170–177, Porto, Portugal.

Faverjon, B. and Tournassoud, P. (1987). A local based approach for path planning of manipulators with a high number of degrees of freedom. In *Proc. IEEE Int. Conf. Robotics and Automation*, volume 4, pages 1152–1159, Raleigh, NC, USA.

Han, J. and Chung, W. K. (2007). Redundancy resolution for underwater vehicle-manipulator systems with minimizing restoring moments. In *Proc. IEEE/RSJ Int. Conf. Intelligent Robots and Systems IROS 2007*, pages 3522–3527, San Diego, CA, USA.

Kanoun, O., Lamiraux, F., and Wieber, P. B. (2011). Kinematic control of redundant manipulators: generalizing the task-priority framework to inequality task. *IEEE Transactions on Robotics*, 27(4):785–792.

Khatib, O. (1987). A unified approach for motion and force control of robot manipulators: The operational space formulation. *IEEE Journal on Robotics and Automation*, 3(1):43–53.

Lane, D. M., Davies, J. B. C., Casalino, G., Bartolini, G., Cannata, G., Veruggio, G., Canals, M., Smith, C., O'Brien, D. J., Pickett, M., Robinson, G., Jones, D., Scott, E., Ferrara, A., Angelleti, D., Coccoli, M., Bono, R., Virgili, P., Pallas, R., and Gracia, E. (1997). AMADEUS: advanced manipulation for deep underwater sampling. *IEEE Robot Autom Mag*, 4(4):34–45.

Macjeiesky, A. A. and Klein, C. A. (1985). Obstacle avoidance for kinematically redundant manipulators in dynamically varying environments. *International Journal of Robotic Research*, 4(5):109–117.

Mansard, N., Khatib, O., and Kheddar, A. (2009a). A unified approach to integrate unilateral constraints in the stack of tasks. *IEEE Trans. Robot.*, 25(3):670–685.

Mansard, N., Remazeilles, A., and Chaumette, F. (2009b). Continuity of varying-feature-set control laws. *IEEE Trans. on Automatic Control*, 54(11):2493–2505.

Marani, G., Choi, S. K., and Yuh, J. (2008). Underwater autonomous manipulation for intervention missions AUVs. *Ocean Engineering*, 36:15–23.

McCain, H., Andary, J., Hewitt, D., and Spidaliere, P. (1991). Flight telerobotic servicer: the design and evolution of a dexterous space telerobot. In *Telesystems Conference, 1991. Proceedings. Vol.1., NTC '91., National*, pages 385–390, Atlanta, GA, USA.

Nakamura, Y. (1991). *Advanced Robotics: Redundancy and Optimization*. Addison Wesley.

Padir, T. (2005). Kinematic redundancy resolution for two cooperating underwater vehicles with on-board manipulators. In *Proc. IEEE Int Systems, Man and Cybernetics Conf*, volume 4, pages 3137–3142, Waikolo, HI, USA.

Schempf, H. and Yoerger, D. (1992). Coordinated vehicle/manipulator design and control issues for underwater telemanipulation. In *IFAC Control Applications in Marine Systems (CAMS 92)*, pages 259–267, Genova, Italy.

Sentis, L. and Khatib, O. (2005). Control of free-floating humanoid robots through task prioritization. In *Proceedings of the 2005 IEEE International Conference on Robotics & Automation*, pages 1718–1723, Barcelona, Spain.

Siciliano, B., Sciavicco, L., Villani, L., and Oriolo, G. (2009). *Robotics: modelling, planning and control*. Springer.

Siciliano, B. and Slotine, J.-J. E. (1991). A general framework for managing multiple tasks in highly redundant robotic systems. In *Proc. Fifth Int Advanced Robotics 'Robots in Unstructured Environments', 91 ICAR. Conf*, pages 1211–1216, Pisa, Italy. IEEE.

Simetti, E., Turetta, A., and Casalino, G. (2009). Distributed control and coordination of cooperative mobile manipulator systems. In Asama, H., Kurokawa, H., Ota, J., and Sekiyama, K., editors, *Distributed Autonomous Robotic Systems 8*, pages 315–324. Springer Berlin Heidelberg.

Spofford, J. R. and Akin, D. L. (1990). Redundancy control of a free-flying telerobot. *Journal of Guidance, Control, and Dynamics*, 13(3):515–523.

Sugiura, H., Gienger, M., Janssen, H., and Goerick, C. (2007). Real-time collision avoidance with whole body motion control for humanoid robots. In *Proc. IEEE/RSJ Int. Conf. Intelligent Robots and Systems IROS 2007*, pages 2053–2058, San Diego, CA, USA.

Yoerger, D. R., Schempf, H., and DiPietro, D. M. (1991). Design and performance evaluation of an actively compliant underwater manipulator for full-ocean depth. *Journal of Robotic Systems*, 8(3):371–392.

Yoshikawa, T. (1984). Analysis and control of robot manipulators with redundancy. In Brady, M. and R.Paul, editors, *Robotic Research: The First International Symposium*, pages 735–747. MIT Press.

Yoshikawa, T. (1985). Manipulability of robotic mechanisms. *Int. J. of Robotics Research*, 4(1):3–9.

Yuh, J. (2000). Design and control of autonomous underwater robots: A survey. *Autonomous Robots*, 8(1):7–24.

Yuh, J., Choi, S., Ikehara, C., Kim, G., McMurty, G., Ghasemi-Nejhad, M., Sarkar, N., and Sugihara, K. (1998). Design of a semi-autonomous underwater vehicle for intervention missions (SAUVIM). In

Underwater Technology, 1998. Proceedings of the 1998 International Symposium on, pages 63–68, Tokyo, Japan. IEEE.